



# Geophysical Research Letters

## RESEARCH LETTER

10.1029/2019GL086933

### Key Points:

- Catastrophic flooding over the Missouri and Mississippi River basins in spring 2019 triggered wet soils and reduced boundary layer depths
- We compared our findings with climatological patterns to study the anomalies in soil moisture, soil temperature, and boundary layer depth
- The interplay between soil moisture and boundary layer depth changes provided a new opportunity to study land-atmosphere feedback

### Supporting Information:

- Supporting Information S1
- Figure S1
- Figure S2
- Figure S3
- Figure S4
- Figure S5
- Figure S6
- Figure S7
- Figure S8
- Figure S9
- Figure S10

### Correspondence to:

S. Pal,  
sandip.pal@ttu.edu

### Citation:

Pal, S., Lee, T. R., & Clark, N. E. (2020). The 2019 Mississippi and Missouri River flooding and its impact on atmospheric boundary layer dynamics. *Geophysical Research Letters*, 47, e2019GL086933. <https://doi.org/10.1029/2019GL086933>

Received 31 DEC 2019  
Accepted 4 MAR 2020  
Accepted article online 12 MAR 2020

©2020. American Geophysical Union.  
All Rights Reserved.

## The 2019 Mississippi and Missouri River Flooding and Its Impact on Atmospheric Boundary Layer Dynamics

Sandip Pal<sup>1</sup> , Temple R. Lee<sup>2,3</sup> , and Nicholas E. Clark<sup>1</sup> 

<sup>1</sup>Department of Geosciences, Atmospheric Science Division, Texas Tech University, Lubbock, TX, USA, <sup>2</sup>Cooperative Institute for Mesoscale Meteorological Studies (CIMMS), Norman, OK, USA, <sup>3</sup>NOAA Air Resources Laboratory Atmospheric Turbulence and Diffusion Division, Oak Ridge, TN, USA

**Abstract** In spring 2019, a catastrophic flood occurred along the Missouri and Mississippi River basins in the United States, which was characterized as the longest lasting flood since the Great Flood of 1927. The 2019 flooding resulted in extremely wet soils for 3–4 months over the Great Plains. Using rawinsonde-derived atmospheric boundary layer depths (BLDs) and in situ soil moisture (SM) data sets at 10 sites located meridionally across the two river-valleys, we investigated the SM controls on regional-scale BLDs during spring 2019. The impact of spring flooding on atmospheric boundary layer dynamics is reported via regression analyses between daily SM and BLDs yielding statistically significant negative  $r$  ( $p < 0.0012$ ) with substantial spatial variability ( $r$ :  $-0.25$  to  $-0.70$ ). Results suggest (1) the strengthening of the negative SM-BLD relationship in the wake of extreme flooding and (2) positive SM anomalies of  $0.05\text{--}0.12 \text{ m}^3 \text{ m}^{-3}$  resulted in negative BLD anomalies ( $-100$  to  $-400$  m) compared to 8-year means, confirming the impact of perturbed land atmosphere feedback processes (LAFP). These results offer a test bed for developing better numerical models with advanced representations of LAFP.

**Plain Language Summary** In spring 2019, a significant flood occurred along the Missouri and Mississippi River basins in the United States, causing the soil to remain very wet and saturated at some places for more than 3 months. In the present study, we investigated how the height of Earth's atmospheric boundary layer, which is an important parameter used in weather forecast and air pollution models, varied because of the wet soils in this region. We performed this study using a network of observations obtained from instrumented weather balloons, as well as highly accurate measurements of soil moisture from within the region. We found that the wet soils resulted in smaller boundary layer heights when compared with how boundary layer heights typically behave over the region. The knowledge gained from this work will be used to help us better represent extreme events in weather forecasting models.

## 1. Introduction

In the rapidly changing climate regime of the 21st century, weather and climate phenomena are becoming less distinct, making the atmospheric processes a “continuum,” rather than a process of two separate time scales (e.g., Davy & Esau, 2016; Zhou et al., 2019). Thus, one requires an improved understanding of the connections between weather and climate, for example, when severe weather and natural disasters like flooding, droughts, tornadoes, and hurricanes are becoming more frequent and causing economic damages (Coronese et al., 2019). For instance, over the United States, overall costs due to 254 weather and climate disasters from 1980–2019 exceeded \$1.7 trillion (Smith & Matthews, 2015).

The recent flooding along the Mississippi and Missouri River valleys in the United States during the spring 2019 caused numerous problems, affecting many roads, transportations, businesses, homes, and lives, and caused more than \$1 billion losses in farming, manufacturing, and navigation (NOAA report 2019). The spring-2019 flooding has been found to be the longest-lasting flood since the 1927 Great Flood (Smith & Reed, 1990). For instance, many locations in the Mississippi (MS) River basin remained above flood-stage for more than 153 consecutive days in spring. Gensini et al. (2019) reported May 2019 to be an exceptionally active period for tornadic thunderstorms (e.g., 757 tornado warning, seven fatalities). The Missouri River basin had more runoff in 3 months in spring 2019 than it typically receives in a year (National Weather Service, NWS, 2019a). Significant flooding mainly occurred on the mainstream Mississippi due to snowmelt in the Northern Great Plains, frozen ground, spring rainfall, and saturated soils. These flooding regimes and associated meteorological conditions cumulatively influenced the soil-moisture (SM) regimes over large

portions of the Great Plains. In addition to the damages to buildings, transportation, life, and property losses, the spring flooding caused a delay in planting different crops in many portions of the United States (e.g., NWS, 2019a, 2019b; USDA, 2019).

SM is a critical bio-geophysical parameter governing land-atmosphere feedback process (LAFP; Jensen, 1983). The role of SM in modulating atmospheric boundary layer (ABL) dynamics, in particular ABL depths (henceforth, BLDs), has been reported before (e.g., Ek & Mahrt, 1994; Liu & Pu, 2019). Several researchers illustrated that increases in precipitation increase available SM, thereby causing higher (lower) latent (sensible) heat fluxes (e.g., Koster et al., 2004; Pal & Haeffelin, 2016) through the effects of SM on evaporation and transpiration, resulting in reduced BLD growth rate (Ek & Mahrt, 1994). Some others investigated the feedback between precipitation and SM for drought and flooding (e.g., Trenberth & Guillemot, 1996; Zhou et al., 2019). However, a detailed investigation of ABL dynamics under extreme flooding conditions and associated changes in SM and LAFP is important since the interaction among surface evaporation, SM, and BLD variability is complex (Findell & Eltahir, 2003). Since rawinsonde measurements provide a “snapshot view” of ABL and do not provide any information about the BLD growth rate, this study aims to explore the SM-BLD relationship.

The spatiotemporal variability in the perturbed land-surface properties due to SM changes can generate mesoscale convergence lines, which can impact convection initiation (CI) (Garcia-Carreras et al., 2010). Additionally, SM anomalies may lead to precipitation anomalies over an extended region via horizontal variability in fluxes, mesoscale circulations, and CI (e.g., Seneviratne et al., 2010; Taylor, 2015). Dirmeyer et al. (2013) illustrated SM-precipitation feedbacks, whereas Halder et al. (2015) outlined the need for both advanced LAFP and observations in simulating hydroclimatic variability over an extended region. Understanding of the ABL kinematics and thermodynamic features under extreme wet regime and associated LAFP is important since ABL features modulate numerous atmospheric processes, for example, CI, aerosol-cloud microphysics, and turbulent mixing of aerosols and pollutants (e.g., An et al., 2019; Dirmeyer & Halder, 2016, 2017). Furthermore, the precipitation-SM feedback process involves multiple non-linear interactions among soil-water storage, runoff, evapotranspiration, orographic features, vegetation cover, and precipitation types (Schubert et al., 2004). The precipitation-SM relationship further impacts the variability in energy balance, evapotranspiration, and BLD variability (e.g., Barthlott & Kalthoff, 2011; Niroula et al., 2018).

The key mechanism of LAFP governing meteorological conditions and ABL dynamics are understood reasonably well (e.g., Betts et al., 1996; Ek & Holtslag, 2004). However, most of the fundamental research work on the LAFP involves SM control on BLD features under fair weather conditions, drought, and during surface-driven CI regimes without considering the nexus between anomalous SM and BLDs across a large region for an extended period in response to a significant flooding. This potentially leads to errors and uncertainties in estimations of ABL forcing under extreme weather conditions because, during such events, the LAFP is significantly influenced by the SM regime, specifically the soil and vegetation characteristics and precipitations. Thus, SM is known to have a longer-lasting effect due to land-surface memory. However, the extent of these interactions and their implications for LAFP on ABL dynamics is not yet fully understood. It is not clear how the excessive wet-soil conditions and surface forcing influence meteorological processes, leading to spatiotemporal BLD variability. Furthermore, no empirical research has yet been performed to investigate the impact of extreme flooding conditions on the BLD variability over an extended region as the US Great Plains.

We hypothesize that anomalously high precipitation and wet-soil conditions affect BLDs for an extended period during, and in response to, immense flooding and the dependence of BLDs on the SM-variability changes spatially and temporally. To investigate the impact of perturbed LAFP on ABL dynamics under anomalously wet regimes, we explored rawinsonde-derived BLDs in March, April, May, and June (MAMJ) for the period 2011–2019 over the 10 selected Integrated Global Radiosonde Archive (IGRA) sites located along the Mississippi and Missouri River valleys (Figure 1 and Table S1 in the supporting information). We also explored volumetric SM (i.e., fractional-volumetric water content,  $\text{m}^3 \text{ m}^{-3}$ , henceforth referred to as SM) variability at 10 U.S. Climate Reference Network (USCRN) sites (Diamond et al., 2013). Note that an investigation of the impact of the perturbed LAFP on the convection initiation (Yin et al., 2015) remains beyond the scope of this work.

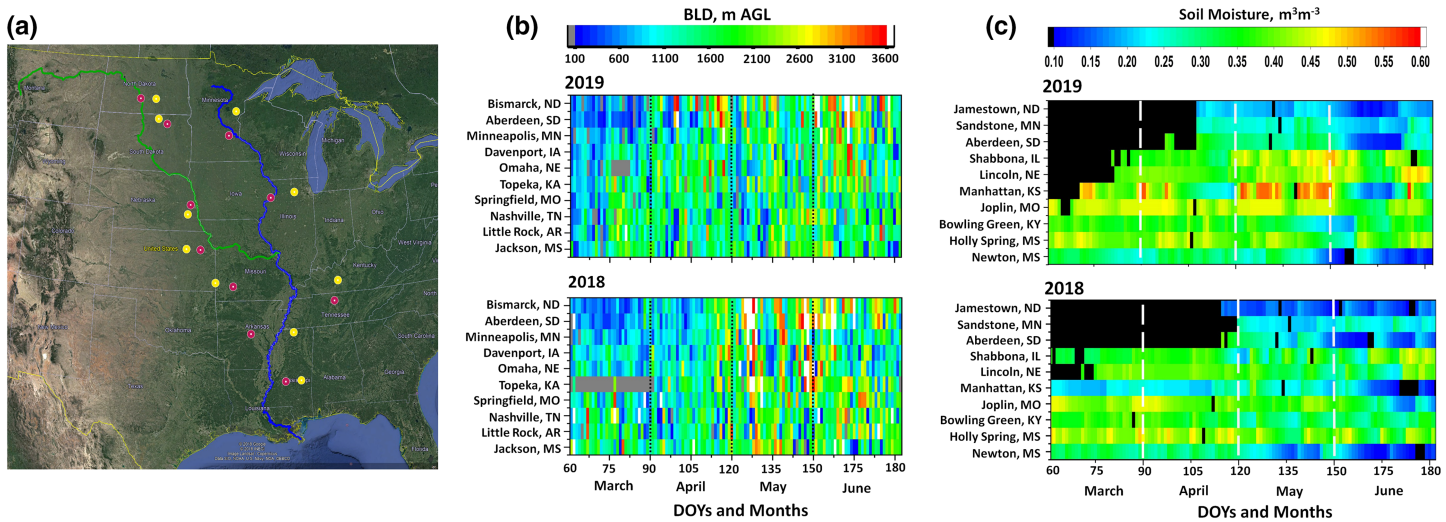


**Figure 1.** (a) Locations of 10 selected IGRA (red circles) and USCRN (yellow circles) sites in the Mississippi River (blue) and Missouri River (green) basins. (b) Heat-map view of the daily afternoon BLDs over the IGRA sites (arranged from south to north in y-axis labels) during MAMJ 2018–2019. Colorbar scales are kept identical (100–3,600 m AGL) for intercomparison. Dotted black lines separate months; gray pixels mark missing data. (c) Same as panel (b) but for daily SM at −5 cm for MAMJ for 2018–2019. Dotted white lines separate months; black pixels mark missing data. Color-bar scale limits are kept identical for all panels for intercomparison.

Notwithstanding, our work is unique compared to the previous studies in that it (1) exploits cases with season-long BLD features occupying an important space in analyzing LAFFP, as encapsulated by processes such as the detailed SM-BLD relationship; (2) addresses the strengthening of the negative SM-BLD relationship in the wake of extreme flooding; (3) examines the SM-BLD relationship over a broad meridional region like the U.S. Great Plains for an extended period, supporting the robustness of the results; (4) demonstrates the concept of a “network of network” by combining routine observations from two networks (i.e., IGRA for thermodynamic profiles and USCRN for SM variability) to illustrate a process-based understanding on the SM-BLD relationship; and (5) explores SM-BLD relationship on both weather scale (day-to-day variability) and climatological scale (anomalous features with respect to short-term and long-term climatologies).

## 2. Data and Methods

We used routine late-afternoon (00-UTC) rawinsonde observations obtained from the IGRA database (Durre et al., 2006) and near-surface meteorological observations from the nearby USCRN sites (Bell et al., 2013). Each USCRN site uses a triple-redundancy approach for SM measurements at five different depths (−5, −10, −20, −50, and −100 cm), and the data are rigorously quality controlled to ensure an accurate data set. The USCRN sites are located in areas with similar surface characteristics surrounding each station (i.e., mostly grassland; Table S1), and the sites have similar soil characteristics. Among the USCRN sites used in this study, the mean wilting point and field capacity was  $11.7\% \pm 3.3\%$  and  $26.4\% \pm 6.1\%$ , respectively. While making the selection of these sites, we ensured that the IGRA sites were (1) far enough from the coast so that the impact of the marine boundary layer was negligible (Pal & Lee, 2019a) and (2) not influenced by the elevated mixed-layer off mountains (Pal & Lee, 2019b). The distance between the IGRA and USCRN sites varies from 58–258 km (Table S1). We used daily SM measurements (−5 and −10 cm), which lacked major data gaps at the 10 USCRN sites during MAMJ (2011–2019).

We estimated the daily afternoon BLDs from the 00 UTC soundings over the 10 sites (Figure 1a) using a recently developed method based on the analyses of bulk Richardson number ( $Ri_b$ ) (Koffi et al., 2016; Lee & De Wekker, 2016; Lee & Pal, 2017). From the profile of  $Ri_b$ , we estimated the ABL top as the height at which the  $Ri_b$  first exceeded 0.25 (e.g., Vogelegen & Holtslag, 1996). The method used (i.e., Lee et al., 2018; Lee & De Wekker, 2016; Pal et al., 2016) reduces uncertainties related to shallow BLDs by removing near-surface stable layers. Thus, BLDs derived using the improved  $Ri_b$  approach represent good estimates of the quasi-stationary afternoon maximum BLD (see Lee & De Wekker, 2016).

Combining measurements from both networks (i.e., IGRA and USCRN) provided us with an exceptional data set to examine the relationship between BLD and SM during the spring-2019 flooding. The heat-map views of the total monthly precipitation and normalized monthly means of SM at 10 USCRN sites during MAMJ for the period 2016–2019 confirmed higher amounts of precipitation and consequently wet conditions in spring 2019 compared to the previous years (Figures S1 and S2).

### 3. Results and Discussion

The classical relationship between the SM at different depths and near-surface meteorological parameters has been extensively reported in the past literature (e.g., Ek & Holtslag, 2004; Liu & Pu, 2019; Santanello et al., 2009, 2011). However, we are mainly interested in the SM controls on the BLDs during an extensive flooding event, which is rare in the literature. To examine the impact of MS and Missouri (MO) river flooding and associated LAFP on the BLD variability, we performed the following analyses: (1) investigation of spatiotemporal variability of BLDs and SM over the 10 paired sites during spring 2019; (2) determination of anomalous characteristics in BLDs and SM compared to their short-term (2016–2018) and long-term (2011–2018) regional-scale climatological patterns due to the spring flooding to examine biases in the findings of the short-term climatology (if any); (3) regression analyses between daily BLDs and SM over the 10 sites for MAMJ for the period 2016–2019 for obtaining the spatial variability in SM-BLD relationship; and (4) regression between monthly-mean BLD and SM anomalies with respect to their 8-year means for MAMJ to quantify the impact of perturbed SM on BLDs. We were unable to present decadal-climatological patterns in both parameters because SM measurements were unavailable prior to 2011.

#### 3.1. Spatiotemporal Variability of BLDs and SM

To investigate spatiotemporal variability in BLDs during spring-2019 flooding conditions, we first explored the overall BLD variability over the 10 sites during MAMJ as presented via a heat map view of the daily afternoon BLDs (e.g., Figure 1b for 2018–2019). Results show that BLDs over most of the sites in spring 2019, in particular in March and May, were generally shallower compared to the other 3 years. The spatial variability of monthly-mean BLDs over these sites also corroborate this feature (Figure S3).

Furthermore, we analyzed daily SM observations at –5 and –10 cm at the 10 USCRN sites for MAMJ of 2018–2019 (see Figure 1c for –5 cm and Figure S4 for –10 cm). The USCRN sites are arranged according to their locations (i.e., latitudes) along the y axis so that they are oriented from south (bottom) to north (top). In general, there exists a stronger interaction between the topsoil moisture and the atmosphere governing LAFP compared to the other deeper soil levels (e.g., Liu & Pu, 2019). We mainly analyzed SM variability at two levels (–5 and –10 cm) because there were significant data gaps in the SM measurements at the other levels (i.e., –20 cm; Figure S7). For example, the data completion for the –5 cm across all sites considered in this study was around 80% but was ~60% or even less for some sites when averaged across all sites for the deeper levels (e.g., –100 cm, not shown). Nevertheless, we performed regression analyses between BLDs and SM at those levels (section 3.4). Despite data gaps at the northern sites (e.g., Aberdeen, Sandstone, and Jamestown), in general, the results reveal wetter soil regime in 2019 compared to 2018 due to flooding. Also, the comparison of the monthly-mean SM (–5 cm) for the period 2016–2019 (Figure S2) and 2011–2019 (Figure S5) suggests the same feature.

#### 3.2. Anomalous BLD and SM Regimes Compared to Climatological Means

To quantify the anomalous features in both BLDs and SM variability over all sites in spring 2019 compared to both short-term (3-year, 2016–2018) and long-term (8-year, 2011–2018) climatologies of both parameters, we considered monthly-mean BLDs and SM at –5 cm (Figure S5). There exists more month-to-month variability in the feedback between monthly means of SM and BLDs for sites in the north than in the south, which we attribute to the site-to-site (i.e., south to north) variability in the BLD seasonality between early versus late spring and early summer of 2019. The anomalies of monthly mean BLDs (Figures 2a and 2b) and SM (Figures 2c and 2d) with respect to 3- and 8-year means illustrate wetter SM and shallower BLD regimes in spring 2019 compared to both short- and long-term climatologies. Similar analyses for SM at –10 and –20 cm are shown in the supporting information (Figures S6 and S7).

In particular, these results (Figure 2) show that, except for Jackson, Little Rock, and Nashville, in May 2019, BLD anomalies were negative, ranging from –200 to –600 m compared to the 3-year means and ranging

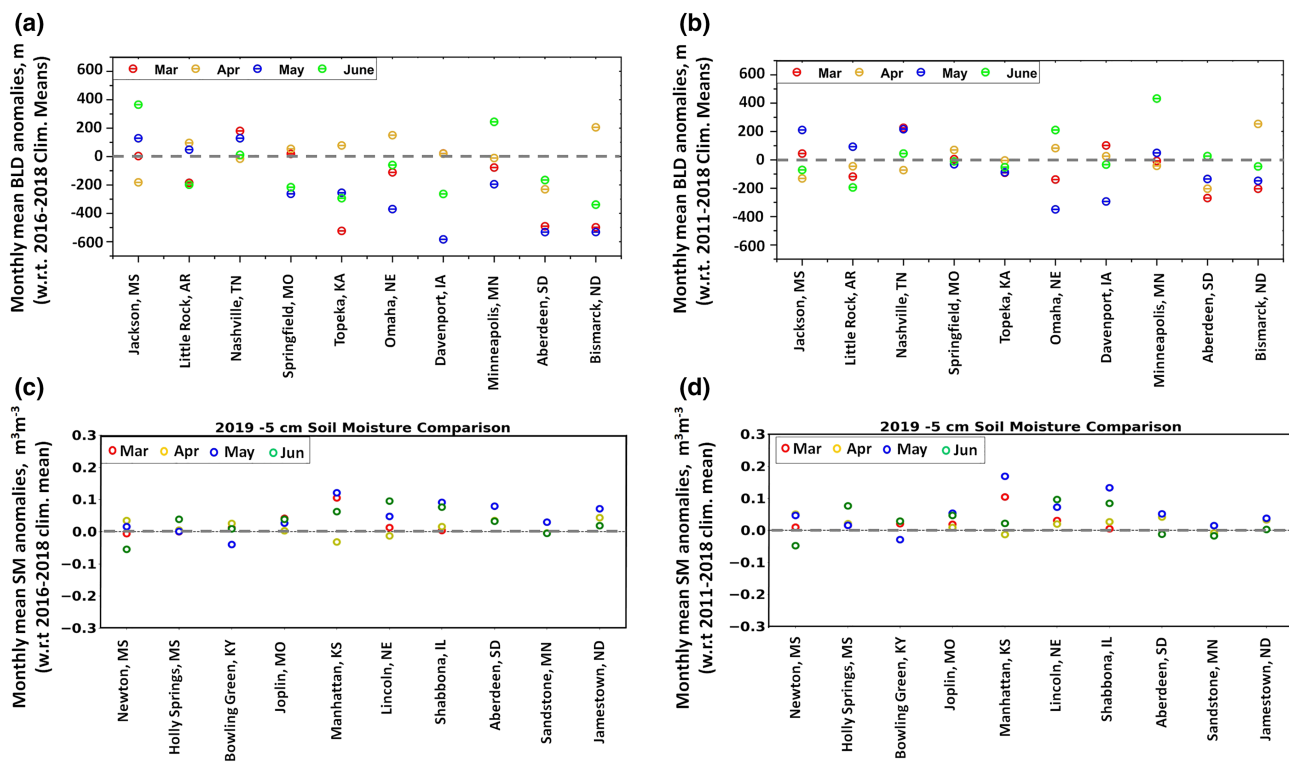


**Figure 2.** Comparisons of monthly-mean BLD anomalies during the months of MAMJ with respect to short-term (3-year, 2016–2018, panel a) and long-term (8-year, 2011–2018, panel b) BLD climatologies of MAMJ for the 10 IGRA sites. Similar analyses for SM (−5 cm) anomalies during MAMJ with respect to short-term (3-year, 2016–2018, panel c) and long-term (8-year, 2011–2018, panel d) SM climatologies of MAMJ for the 10 USCRN sites. The horizontally aligned gray dashed line on each panel marks the zero line indicating no anomalies.

from −100 to −400 m compared to the 8-year means, whereas nearby USCRN sites (except Newton, Holly Springs, and Bowling Green) yielded positive SM anomalies for both short-term (2016–2018) and long-term (2011–2018) climatologies. The distance between these three paired sites varies from 100–258 km (Table S1).

### 3.3. Dependence of BLDs on SM During Spring (2016–2019)

To attribute the dependence of spatial variability (i.e., site-to-site) of BLDs on SM (−5 cm), we first performed linear regressions between daily BLDs and SM at 10 sites during MAMJ of 2016–2019 (Figure 3a). The results of the regression analyses (i.e. heat-map view of  $r$  values) were segregated among different months of spring so that the SM-BLD relationship remains independent of month-to-month variability (e.g., early vs. late spring) in both SM and BLDs (if any) instead of performing overall regression analyses between 122 daily samples (4 months) of SM and BLDs in different years.

The heat-map view of  $r$  (i.e., Pearson correlation coefficient) for MAMJ 2016–2019 (Figure 3a) shows that  $r$  values were smallest in spring 2019, varying between −0.25 and −0.75 (statistically significant with  $p < 0.0001$ ), compared to spring of 2016–2018, except for, for example, May 2016 and March 2018. Results show a strengthening of the negative relationship between SM and BLD during and after the flooding in 2019. The stronger negative correlation coefficients for MAMJ of 2019 also represent the BLD dependence on SM on weather scales (i.e., day-to-day variability) during extreme wet regime over all sites due to 2019-spring flooding.

Additionally, the heat-map view of SM and soil temperature (−5 cm) anomalies (Figure S9) also suggest that anomalously high SM conditions triggered higher rates of evaporation and latent heat fluxes, reducing the amount of radiation available to heat the soil. This reduced soil temperatures; thus, anomalously low soil temperature (ST) regimes prevailed during spring 2019. Consequently, the atmospheric conditions over the region were characterized by lower sensible heat flux and shallower BLDs. Thus, these analyses further

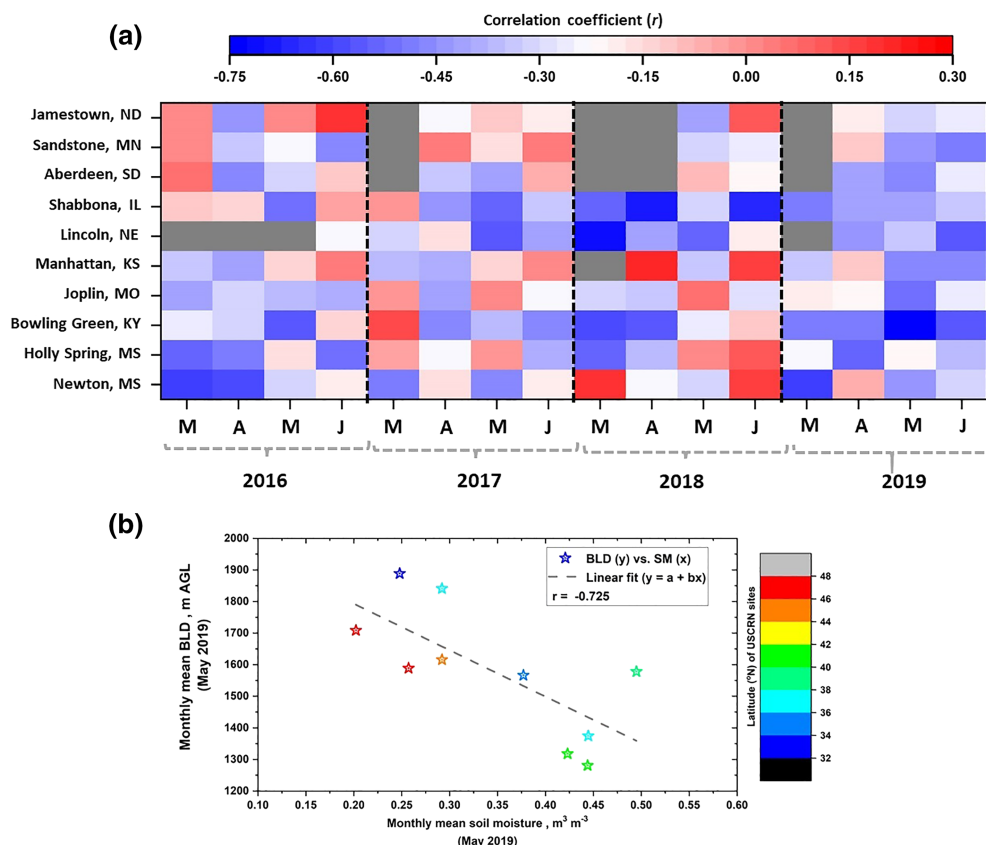


**Figure 3.** (a) Heat-map view of correlation coefficients ( $r$ ) based on daily BLDs and SM ( $-5\text{ cm}$ ) for MAMJ during 2016–2019 illustrating variability in  $r$  (i.e. Pearson correlation coefficient). (b) Scatterplots and regression analysis between monthly-mean BLDs and SM ( $-5\text{ cm}$ ) over the 10 sites for May 2019. Colorbar marks the latitudes of the USCRN (blue: south; red: north).

reinforce the cooling mechanism that positive soil moisture anomalies create, which in turn suppresses BLD growth. Previously, Shukla and Mintz (1982) demonstrated that positive SM anomalies increase evaporation rates and decrease sensible heat flux and BLD growth.

Most likely, the observed site-to-site variability in  $r$  occurred due to the diverse spatial variability in spring precipitation and resultant SM at different sites. However, the correlation between daily SM and BLDs for the paired site Little Rock and Holly Springs was weakest, which we attribute to the largest distance between these two sites (~258 km; Table S1). Whether the observed spatial variability in SM-BLD relationship over the region was further influenced by additional factors (e.g., advection of heat and moisture, entrainment, large-scale subsidence, and mechanically generated turbulence) is a topic for future study.

Nevertheless, results illustrate that the BLD features were not only affected across a large region but also during an extended period. Additionally, to investigate these features in climatological context, we performed regression analysis between monthly-mean BLDs and SM ( $-5\text{ cm}$ ) over the 10 sites for May 2019 (Figure 3b) and found stronger negative correlations for spring 2019 compared to the other years (Figure S8). These combined analyses facilitate a test bed for investigating an important aspect of land surface memory and LAFP (i.e., SM control on BLDs) in the transition beyond weather time scales. Also, the findings suggest the dependence of spatial BLD variability on the underlying SM regimes (i.e., statistically significant negative  $r$ ) over 10 sites during, and in response to, immense flooding illustrating sustained, season-long modification of BLDs associated with negative SM anomalies.

### 3.4. Overall BLD Dependence on SM

Finally, we performed regression analyses between the anomalies of monthly-mean SM at  $-5\text{ cm}$  and BLDs (compared to both 3- and 8-year climatologies) during MAMJ (4 months over 10 sites yielding 40 samples)

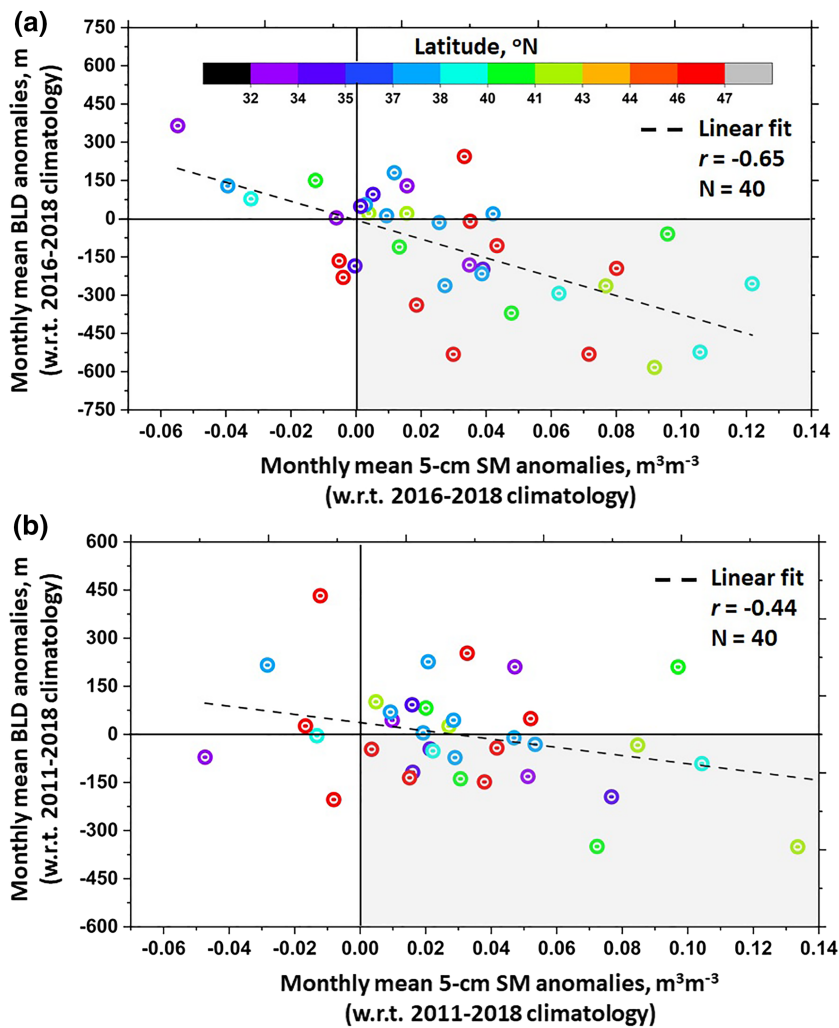


**Figure 4.** (a) Regression analyses between anomalies (with respect to a 3-year climatology, 2016–2018) of monthly-mean BLDs versus SM for all sites during MAMJ ( $r = -0.65$ ). Gray-shaded box demarcates the co-occurring regime of anomalously wet SM and shallow BLDs in MAMJ compared to a 3-year climatology. The horizontally and vertically aligned two black solid lines indicate zero anomalies of BLDs and SM, respectively, whereas the dashed gray line shows the linear fit. (b) Same as (a) but using an 8-year climatology ( $r = -0.44$ ). Colorbar scales (latitudes of USCRN sites) are identical in both panels.

via classifying the SM and BLD features into two broad categories: positive and negative SM (BLD) anomalies indicating wetter and drier (deeper and shallower) than the 3-year means (Figure 4a) and the 8-year means (Figure 4b). These analyses illustrated the overall impact of perturbed SM regime on BLDs and served as an unconstrained verification of the SM control on BLDs under wet conditions, as the anomalies of both parameters remained independent of the seasonal cycle impact (if any) since monthly means were subtracted when calculating the anomalies (Pan & Mahrt, 1987). We found  $r$  (Pearson correlation coefficient) of  $-0.65$  and  $-0.44$  (statistically significant with  $p < 0.0013$  and  $p < 0.0014$ ) for short- and long-term climatologies, respectively, which demonstrates that anomalously wet-soil regimes (demarcated by the gray-shaded box on Figure 4) yield shallower BLDs over the entire region during spring 2019. Additionally, we explored anomalies of deeper SM data sets (i.e.,  $-20$ ,  $-50$ , and  $-100$  cm) compared to 8-year climatological means and presented similar regression analyses between BLD and SM anomalies (Figure S10). As mentioned before, data gaps at  $-20$ ,  $-50$ , and  $-100$  cm layers hampered the analyses (see panels b-d of Figure S10) so that no conclusive results were found except for  $-10$  cm where we obtained a correlation coefficient  $-0.33$  ( $N$  of 37,  $p < 0.0014$ ).

Due to both rapidly changing climate and threats for more frequent floods (e.g., Woldemeskel & Sharma, 2016), several researchers emphasized the requirement for a conceptual framework to connect extreme precipitation features over extended regions and consequent flooding for studying the impact of perturbed LAFP on BLD variability (e.g., Coronese et al., 2019; Wright et al., 2019). In fact, the spring-2019 flooding over the Great Plains could serve as a good case study and holds potential for future investigations of how LAFP are parameterized in weather and climate models (Maxwell et al., 2007). Nonetheless, detailed analyses on these aspects remain sparse in the literature, and, for the first time, we provided empirical evidence on the impact of an extensive flooding and associated SM regime on regional-scale BLD variability. We found a significant impact of the spring-2019 flooding on the BLDs over multiple sites located in the two river basins. Also, the analyses highlight the importance of weather and climate processes becoming less distinguishable and affecting each other as we showed implications for perturbed SM regime on BLDs in response to significant flooding. The results reported here have significant implications for future research as we established an important aspect of LAFP encapsulated by a mechanism such as the SM-BLD relationship under perturbed conditions due to an extreme flooding event. This work provides empirical evidence for validating hydrological models and subseasonal forecasting skills (Hirsch et al., 2014).

#### 4. Concluding Remarks

The Missouri and Mississippi River basins in spring 2019 stands as one of the most catastrophic flooding in the history and was comparable to the 1927 Great Flood. In particular, spring 2019 was characterized by extreme precipitation and severe weather (e.g., bomb cyclones and record number of tornadoes), encompassing a wide region of the MS and MO River basins. We presented the SM-BLD relationship on both weather scale via regression analyses based on day-to-day variability in SM and BLDs, and in a climatological context via examining the anomalous features in SM and BLDs with respect to both short-term (3-year) and long-term (8-year) climatologies.

Within this first-of-its-kind empirical study based on the analyses of rawinsonde-derived BLDs and USCRN volumetric SM observations, we found that regional-scale BLDs over both river basins were anomalously lower ( $-100$  and  $-400$  m) compared to the 8-year climatological means, caused by extremely wet conditions as confirmed by positive SM anomalies ( $0.05\text{--}0.11 \text{ m}^3 \text{ m}^{-3}$ ) over an extended region (e.g., Dirmeyer & Halder, 2016). We found  $r$  of  $-0.65$  ( $-0.44$ ) while performing regression analyses between BLD and SM anomalies with respect to 3-year (8-year) spring climatologies over all sites. This work utilizes multiple data sets to identify meaningful physical relationships between SM and BLD and analyzes the relationship over multiple temporal scales. Our results offer an appropriate test bed for investigating LAFP under extreme weather conditions to investigate the impact of perturbed SM regimes on BLD features on daily, synoptic, and seasonal time scales. During the present rapidly warming climate regime in which time scales of weather and climate processes are converging, we strongly believe that the analyses reported here promise a strong foundation for further work. For instance, one could perform regional climate simulations for LAFP, in particular the SM-BLD relationship, related to severe flooding.

The analyses presented here also demonstrated the potential of combining routine observations from two completely different national networks (i.e., IGRA and USCRN) and consequently helped identify important facets of the SM-BLD relationship over 10 sites oriented meridionally across two major river valleys in response to an immense flooding. Thus, we introduced the concept of a “network of networks” to explore the impact of catastrophic 2019 flooding on the regional-scale BLD variability.

#### References

- An, N., Pinker, R. T., Wang, K., Rogers, E., & Zuo, Z. (2019). Evaluation of cloud base height in the North American regional reanalysis using ceilometer observations. *International Journal of Climatology*, 1–19. <https://doi.org/10.1002/joc.6389>
- Barthlott, C., & Kalthoff, N. (2011). A numerical sensitivity study on the impact of soil moisture on convection-related parameters and convective precipitation over complex terrain. *Journal of the Atmospheric Sciences*, 68(12), 2971–2987. <https://doi.org/10.1175/JAS-D-11-0271>
- Bell, J. E., Palecki, M. A., Baker, C. B., Collins, W. G., Lawrimore, J. H., Leeper, R. D., et al. (2013). U.S. climate reference network soil moisture and temperature observations. *Journal of Hydrometeorology*, 14, 977–988. <https://doi.org/10.1175/JHM-D-12-0146.1>
- Betts, A. K., Ball, J. H., Beljaars, A., Miller, M. J., & Viterbo, P. A. (1996). The land surface atmosphere interaction: A review based on observational and global modeling perspectives. *Journal of Geophysical Research*, 101, 7209–7225. <https://doi.org/10.1029/95JD02135>

#### Acknowledgments

This work was sponsored by an internal start-up research grant at TTU, and the co-author NC was funded by TTU PI<sup>2</sup> scholarship. The results and conclusions, and any views expressed herein, are those of the authors and do not necessarily reflect those of NOAA or the Department of Commerce. The IGRA rawinsonde data and USCRN data were obtained online (from <ftp://ftp.ncdc.noaa.gov/> and <https://www.ncdc.noaa.gov/crn/qcdatasets.html>). We thank the two anonymous reviewers for their constructive comments and helpful suggestions. We also thank Ms. Lori Lightfoot (Lead Administrator - Undergraduate Research Scholars at TTU), Ms. Julie Isom (Associate Director for Undergraduate Research) and Dr. Michael San Francisco (Dean of the Honors College, TTU) for their encouragement and support.

- Coronese, M., Lamperti, F., Keller, K., Chiaromonte, F., & Roventini, A. (2019). Evidence for sharp increase in the economic damages of extreme natural disasters. *Proceedings of the National Academy of Sciences*, 116(43), 21,450–21,455. <https://doi.org/10.1073/pnas.1907826116>
- Davy, R., & Esau, I. (2016). Differences in the efficacy of climate forcings explained by variations in atmospheric boundary layer depth. *Nature Communications*, 7(1), 1–8. <https://doi.org/10.1038/ncomms11690>
- Diamond, H. J., Karl, T. R., Palecki, M. A., Baker, C. B., Bell, J. E., Leeper, R. D., et al. (2013). U.S. Climate Reference Network after one decade of operations: Status and assessment. *Bulletin of the American Meteorological Society*, 94, 489–498. <https://doi.org/10.1175/BAMS-D-12-00170.1>
- Dirmeyer, P. A., & Halder, S. (2016). Sensitivity of numerical weather forecasts to initial soil moisture variations in CFSv2. *Weather and Forecasting*, 31(6), 1973–1983. <https://doi.org/10.1175/WAF-D-16-0049.1>
- Dirmeyer, P. A., & Halder, S. (2017). Application of the land-atmosphere coupling paradigm to the operational Coupled Forecast System, Version 2 (CFSv2). *Journal of Hydrometeorology*, 18(1), 85–108. <https://doi.org/10.1175/JHM-D-16-0064.1>
- Dirmeyer, P. A., Jin, Y., Singh, B., & Yan, X. (2013). Trends in land-atmosphere interactions from CMIP5 simulations. *Journal of Hydrometeorology*, 14(3), 829–849. <https://doi.org/10.1175/JHM-D-12-0107.1>
- Durre, I., Vose, R., & Wuertz, D. (2006). Overview of the integrated global radiosonde archive. *Journal of Climate*, 19, 53–68. <https://doi.org/10.1175/JCLI3594.1>
- Ek, M., & Holtslag, A. (2004). Influence of soil moisture on boundary layer cloud development. *Journal of Hydrometeorology*, 5, 86–99. [https://doi.org/10.1175/1525-7541\(2004\)005<0086:IOSMOB>2.0.CO;2](https://doi.org/10.1175/1525-7541(2004)005<0086:IOSMOB>2.0.CO;2)
- Ek, M., & Mahrt, L. (1994). Daytime evolution of relative humidity at the boundary layer top. *Monthly Weather Review*, 122, 2710–2721. [https://doi.org/10.1175/1520-0493\(1994\)122<2709:DEORHA>2.0.CO;2](https://doi.org/10.1175/1520-0493(1994)122<2709:DEORHA>2.0.CO;2)
- Findell, K. L., & Eltahir, E. A. B. (2003). Atmospheric controls on soil moisture-boundary layer interactions: Three-dimensional wind effects. *Journal of Geophysical Research*, 108(D8), 8385. <https://doi.org/10.1029/2001JD001515>
- Garcia-Carreras, L., Parker, D. J., Taylor, C. M., Reeves, C. E., & Murphy, J. G. (2010). Impact of mesoscale vegetation heterogeneities on the dynamical and thermodynamic properties of the planetary boundary layer. *Journal of Geophysical Research*, 115, D03102. <https://doi.org/10.1029/2009JD012811>
- Gensini, V. A., Gold, D., Allen, J. T., & Barrett, B. S. (2019). Extended U.S. tornado outbreak during late May 2019: A forecast of opportunity. *Geophysical Research Letters*, 46, 10,150–10,158. <https://doi.org/10.1029/2019GL084470>
- Halder, S., Dirmeyer, P. A., & Saha, S. K. (2015). Uncertainty in the mean and variability of Indian summer monsoon due to land-atmosphere feedback in RegCM4. *Journal of Geophysical Research: Atmospheres*, 120, 9437–9458. <https://doi.org/10.1002/2015JD023101>
- Hirsch, A. L., Kala, J., Pitman, A. J., Carouge, C., Evans, J. P., Haverd, V., & Mocko, D. (2014). Impact of land surface initialization approach on subseasonal forecast skill: A regional analysis in the Southern Hemisphere. *Journal of Hydrometeorology*, 15, 300–319. <https://doi.org/10.1175/JHM-D-13-05.1>
- Jensen, J. R. (1983). Biophysical remote sensing. *Annals of the Association of American Geographers*, 73, 111–132. <https://www.jstor.org/stable/2569349>
- Koffi, E. N., Bergamaschi, P., Karstens, U., Krol, M., Segers, A., Schmidt, M., et al. (2016). Evaluation of the boundary layer dynamics of the TM5 model over Europe. *Geoscientific Model Development*, 9(9), 3137–3160. <https://doi.org/10.5194/gmd-9-3137-2016>
- Koster, R. D., Dirmeyer, P. A., & Guo, Z. C. (2004). Regions of strong coupling between soil moisture and precipitation. *Science*, 305(5687), 1138–1140. <https://doi.org/10.1126/science.1100217>
- Lee, T. R., & De Wekker, S. F. J. (2016). Estimating daytime planetary boundary layer heights over a valley from rawinsonde observations at a nearby airport: An application to the Page Valley in Virginia, USA. *Journal of Applied Meteorology and Climatology*, 55(3), 791–809. <https://doi.org/10.1175/JAMC-D-15-0300.1>
- Lee, T. R., De Wekker, S. F. J., & Pal, S. (2018). The impact of the afternoon planetary boundary-layer height on the diurnal cycle of CO and mixing ratios at a low-altitude mountaintop. *Boundary-Layer Meteorology*, 168(1), 81–102. <https://doi.org/10.1007/s10546-018-0343-9>
- Lee, T. R., & Pal, S. (2017). On the potential of 25 years (1991–2015) of rawinsonde measurements for elucidating climatological and spatiotemporal patterns of afternoon boundary layer depths over the contiguous US. *Advances in Meteorology*, 1–19. <https://doi.org/10.1155/2017/6841239>
- Liu, J., & Pu, Z. (2019). Does soil moisture have an influence on near-surface temperature? *Journal of Geophysical Research: Atmospheres*, 124, 6444–6466. <https://doi.org/10.1029/2018JD029750>
- Maxwell, R. M., Chow, F. K., & Kollet, S. J. (2007). The groundwater-land-surface-atmosphere connection: Soil moisture effects on the atmospheric boundary layer in fully-coupled simulations. *Advances in Water Resources*, 30(12), 2447–2466. <https://doi.org/10.1016/j.advwatres.2007.05.018>
- Niroula, S., Halder, S., & Ghosh, S. (2018). Perturbations in the initial soil moisture conditions: Impacts on hydrologic simulation in a large river basin. *Journal of Hydrology*, 561, 509–522.
- NWS (National Weather Service) (2019a). Report on Mississippi River Flood History 1543–Present, [https://www.weather.gov/lix/ms\\_flood\\_history](https://www.weather.gov/lix/ms_flood_history) (Online).
- NWS (National Weather Service) (2019b). Report on Spring 2019 flooding. [https://www.weather.gov/dvn/summary\\_SpringFlooding\\_2019](https://www.weather.gov/dvn/summary_SpringFlooding_2019) (Online)
- Pal, S., De Wekker, S. F. J., & Emmitt, G. D. (2016). Investigation of the spatial variability of the convective boundary layer heights over an Isolated Mountain: Cases from the MATERHORN-2012 experiment. *Journal of Applied Meteorology and Climatology*, 55(9), 1927–1952. <https://doi.org/10.1175/JAMC-D-15-0277.1>
- Pal, S., & Haefelin, M. (2016). Forcing mechanisms governing diurnal, seasonal, and inter-annual variability in the boundary layer depths: Five years of continuous lidar observations over a suburban site near Paris. *Journal of Geophysical Research: Atmospheres*, 120, 11,936–11,956. <https://doi.org/10.1002/2015JD023268>
- Pal, S., & Lee, T. R. (2019a). Contrasting air mass advection explains significant differences in boundary layer depth seasonal cycles under onshore versus offshore flows. *Geophysical Research Letters*, 46, 2846–2853. <https://doi.org/10.1029/2018GL081699>
- Pal, S., & Lee, T. R. (2019b). Adverted airmass reservoirs in the downwind of mountains and their roles in overrunning boundary layer depths over the plains. *Geophysical Research Letters*, 46, 10,140–10,149. <https://doi.org/10.1029/2019GL083988>
- Pan, H.-L., & Mahrt, L. (1987). Interaction between soil hydrology and boundary layer development. *Boundary-Layer Meteorology*, 38, 185–202. <https://doi.org/10.1007/BF00121563>
- Santanello, J. A. Jr., Peters-Lidard, C. D., & Kumar, S. V. (2011). Diagnosing the sensitivity of local land-atmosphere coupling via the soil moisture-boundary layer interaction. *Journal of Hydrometeorology*, 12(5), 766–786. <https://doi.org/10.1175/JHM-D-10-05014.1>

- Santanello, J. A., Peters-Lidard, C. D., Kumar, S. V., Alonge, C., & Tao, W.-K. (2009). A modeling and observational framework for diagnosing local land-atmosphere coupling on diurnal time scales. *Journal of Hydrometeorology*, 10, 577–599. <https://doi.org/10.1175/2009JHM1066.1>
- Schubert, S. D., Suarez, M. J., Pegion, P. J., Koster, R. D., & Bacmeister, J. T. (2004). Causes of long-term drought in the U.S. Great Plains. *Journal of Climate*, 17, 485–503. [https://doi.org/10.1175/1520-0442\(2004\)017<0485:COLDIT>2.0.CO;2](https://doi.org/10.1175/1520-0442(2004)017<0485:COLDIT>2.0.CO;2)
- Seneviratne, S. I., Corti, T., Davin, E. L., Hirschi, M., Jaeger, E. B., Lehner, I., et al. (2010). Investigating soil moisture-climate interactions in a changing climate: A review. *Earth-Science Reviews*, 99(3–4), 125–161. <https://doi.org/10.1016/j.earscirev.2010.02.004>
- Shukla, J., & Mintz, Y. (1982). The influence of land surface evapotranspiration on Earth's climate. *Science*, 215(4539), 1498–1501. <https://doi.org/10.1126/science.215.4539.1498>
- Smith, A., & Matthews, J. (2015). Quantifying uncertainty and variable sensitivity within the U.S. billion-dollar weather and climate disaster cost estimates. *Natural Hazards*, 77(3), 1829–1851. <https://doi.org/10.1007/s11069-015-1678-x>
- Smith, D. T., & Reed, D. B. (1990). A centennial survey of American floods: Fifteen significant events in the United States 1890–1990 Fort Worth, TX. *NOAA Technical Memorandum NWS SR*, 133, 51–57.
- Taylor, C. M. (2015). Detecting soil moisture impacts on convective initiation in Europe. *Geophysical Research Letters*, 42, 4631–4638. <https://doi.org/10.1002/2015GL064030>
- Trenberth, K. E., & Guillemot, C. J. (1996). Physical processes involved in the 1988 drought and 1993 floods in North America. *Journal of Climate*, 9, 1288–1298. [https://doi.org/10.1175/1520-0442\(1996\)009<1288:PPITD>2.0.CO;2](https://doi.org/10.1175/1520-0442(1996)009<1288:PPITD>2.0.CO;2)
- United States Department of Agriculture (USDA), National Agricultural Statistics Service, Reports. (June 2019) [https://www.nass.usda.gov/Publications/Reports\\_By\\_Date/index.php](https://www.nass.usda.gov/Publications/Reports_By_Date/index.php)
- Vogelezang, D. H. P., & Holtslag, A. A. M. (1996). Evaluation and model impacts of alternative boundary-layer height formulations. *Boundary Layer Meteorology*, 81, 245–269. <https://doi.org/10.1007/BF02430331>
- Woldemeskel, F., & Sharma, A. (2016). Should flood regimes change in a warming climate? The role of antecedent moisture conditions. *Geophysical Research Letters*, 43, 7556–7563. <https://doi.org/10.1002/2016GL069448>
- Wright, D. B., Bosma, C. D., & Lopez-Cantu, T. (2019). U.S. hydrologic design standards insufficient due to large increases in frequency of rainfall extremes. *Geophysical Research Letters*, 46, 8144–8153. <https://doi.org/10.1029/2019GL083235>
- Yin, J., Albertson, J. D., Rigby, J. R., & Porporato, A. (2015). Land and atmospheric controls on initiation and intensity of moist convection: CAPE dynamics and LCL crossings. *Water Resources Research*, 51, 8476–8493. <https://doi.org/10.1002/2015WR017286>
- Zhou, S., Williams, A. P., Berg, A. M., Cook, B. I., Zhang, Y., Hagemann, S., et al. (2019). Land–atmosphere feedbacks exacerbate concurrent soil drought and atmospheric aridity. *Proceedings of the National Academy of Sciences*, 116(38), 18,848–18,853. <https://doi.org/10.1073/pnas.1904955116>